

Mineral phase changes during weathering of landmine ores : A comparative study of two mines in Yamagata Prefecture, Japan

Shihchun LIN¹, Haruka HATSUKAWA², Kazuo NAKASHIMA³ and Takashi YUGUCHI⁴

1: Jibanshikenjo Co., Ltd., 1-16-2, Kotobashi, Sumida-ku, Tokyo 130-0022, Japan

2: Graduate School of Science and Engineering, Earth Sciences, 1-4-12, Kojirakawa, Yamagata-city, 990-8560, Japan

3: ASN Co. Ltd., 6-6-3, Aoba-ku, Sendai-city, Miyagi, 989-3204, Japan

4: Department of Earth Sciences, Yamagata University, 1-4-12, Kojirakawa, Yamagata-city, 990-8560, Japan

Abstract

As an aid to reducing the burden of mining pollution treatment, we investigated the weathering processes of ores from landmines. We analyzed ore wastes from the Miocene vein-type, Murayama and Fukufune mines, Yamagata Prefecture, by XRD and EPMA, and measured the pH of stream waters around the mines.

Pyrite is abundant in the Murayama mine, and decomposes to Fe^{2+} and SO_4^{2-} ions with oxidation and hydration during weathering. Fe^{2+} ion easily changes to Fe^{3+} ion in the air environment, and Fe^{3+} ion accelerates the decomposition of chalcopyrite, galena and sphalerite. This raises the production of jarosite-series minerals because of the elution of Al, Fe, Pb, Cu as well as P under very low pH. On the other hand, chalcopyrite is rich in the Fukufune mine, and this leads to the abundant occurrence of covellite and cupric sulfates.

Although the mines are similar deposit type, vein-type, and in age, late Miocene, and abandoned in the middle 1960's, their weathering processes are different. The river waters around the mines are acidic due to the hydrolysis of sulfide minerals, especially the decomposition of pyrite. It is important to identify the type of sulfide minerals, especially the amount of pyrite in the ores, in order to treat the metal mine drainage.

Keywords: land deposit, weathering process, pyrite, sulfate minerals

Introduction

The environmental damage caused by mining, which is a negative legacy of mining development, has become a big problem. Heavy metals in mine waste water and polluted smoke via mining processes and refinement destroy the surroundings and lower streams, resulting in serious medical problems (e.g., Shoji and Sugai, 1992; Alpers et al., 2003; Kitagawa, 2006; Singh, 2006). Advanced countries have been controlling pollution since the last century and the damage is decreasing (e.g., METI, 2012), whereas serious pollution problems have been continued in underdeveloped and resource-producing countries (e.g., Ghose, 2002; Trivedi et al., 2010; Lindahl, 2014).

In Japan, many mines once were exploited until the 1980s. Although most of them are closed now, mine waste frequently remains around the abandoned mines, which often contains undesired toxic metals. The mine waste is then exposed to weathering, and heavy metals and acidic water elutes into waste water which causes the environmental problem (e.g., Ito et al., 2010; Matsumoto, 2010). In order to prevent these influences, it is necessary to elucidate the weathering process of ores and ore minerals. The aim of this study is to know the phase change of ore minerals during the oxidizing weathering process through detailed observation of the ore wastes. We collected many ores from various types of deposit, e.g., vein-, Kuroko- and skarn-types, and found that vein-type Murayama and Fukufune mines show contrasting weathered mineral changes, although their original sulfide mineral

assemblages are similar. We will discuss the weathering process of landmines by comparing these two mines.

General Geology

Murayama mine

The Murayama mine is located in the Nishiyama Mining Area, central Yamagata Prefecture (Fig. 1), in which many vein-type deposits such as Nagamatsu, Sachi and Mitate mines occur (Fig. 2). In this area, middle to late Miocene mudstone, siltstone, acidic volcanics and tuffaceous sandstone cover the Cretaceous granite unconformably (Otsu, 1956; YOC, 2016). The mine is composed of a few deposits, which produced mainly Cu and Zn and are included in the basement granite and the Miocene covers of mudstone and tuffs. Mining started from 1915, producing crude ores of 5,984 t Cu and 547 t Zn in 1919, and ending in 1966 (Yamagata Prefecture, 1977). When we surveyed the mining site in 1989, many facilities and tunnels of abandoned mines were exposed (Fig. 3a), and in 2014, most of the facilities was covered with vegetation, and a waste water treatment facility has been operating (Fig. 3b), leaving behind a large deposit of tailing (Fig. 3c).

Fukufune mine

The geology around the Fukufune mine contains mudstone, rhyolitic tuffs and andesitic tuff breccia of Miocene age (Yamagata Prefecture, 1977). The mine is an epithermal vein-type and is located in the rhyolitic tuffs and lavas. The deposit was mined for mainly Cu from around 1940 to 1972, and produced over 2000 t Cu



Fig. 1 Location of the study area.

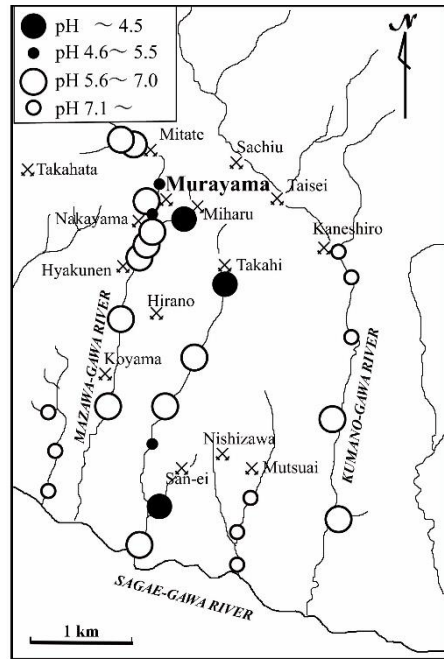


Fig. 2 Distribution of abandoned mines and results of pH measurements in the Nishiyama mining area, central Yamagata Prefecture.

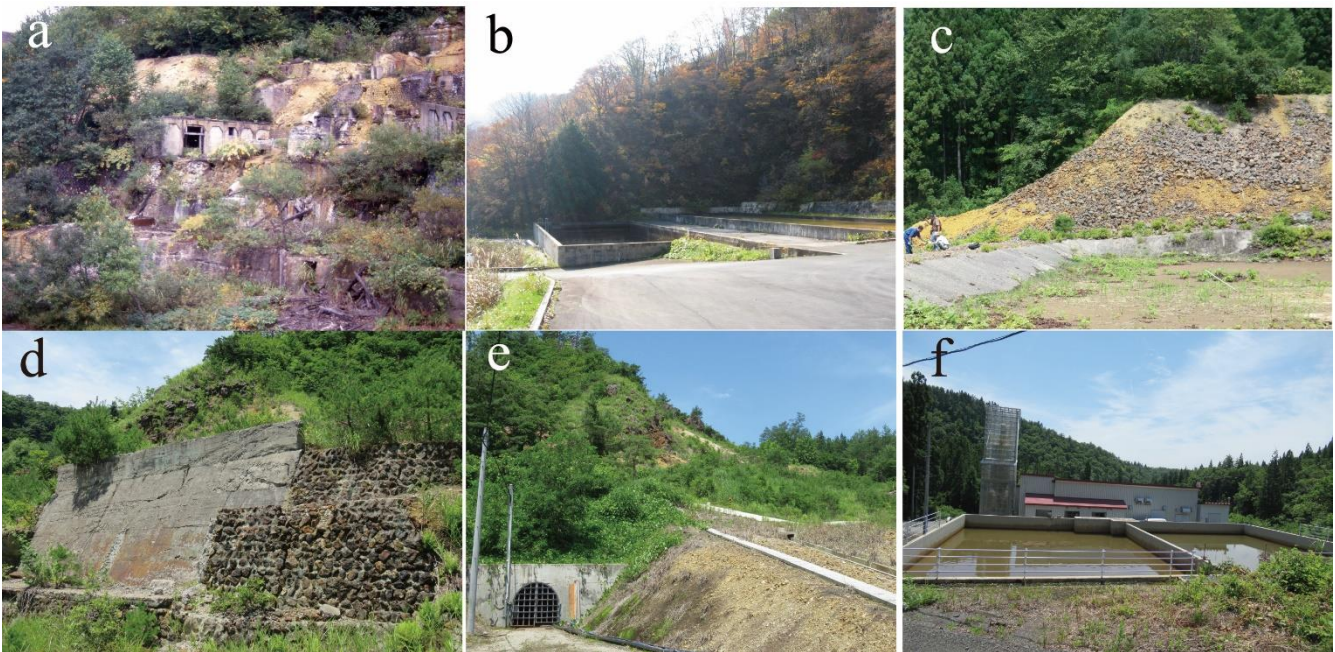


Fig. 3 Photographs of abandoned mine facilities of the Nishiyama mining area and the Fukufune mine, Yamagata Prefecture. a: Abandoned mine facility at the Sachi mine (1989). b: A waste water facility at the Sachi mine (2014). c: A tailing deposit at the Murayama mine (2014). d: A part of mine facilities and stone walls are remaining at the Fukufune mine (2020). e: An adit was covered with the iron fence at the Fukufune mine (2020). f: A waste water treatment facility at the Fukufune mine (2020).

concentrates every year from 1955 to 1967 (Yamagata Prefecture, 1977). In 2016, the mining site was covered with vegetation, and some tailings were scattered on the grass field.

Sample and Methods

Sample

Murayama mine: The host rock of the studied ores is tuff and tuff breccia (Fig. 4a), and suffered from silicification (Fig. 4b) and partly clay (chlorite+kaolinite) alteration. Ores occur as pyrite - quartz vein of less than a few cm wide, sphalerite (+pyrite) - quartz vein, disseminated pyrite in host rock, and brecciated chalcocopyrite + sphalerite + pyrite vein. Pyrite is abundant by the naked eye in

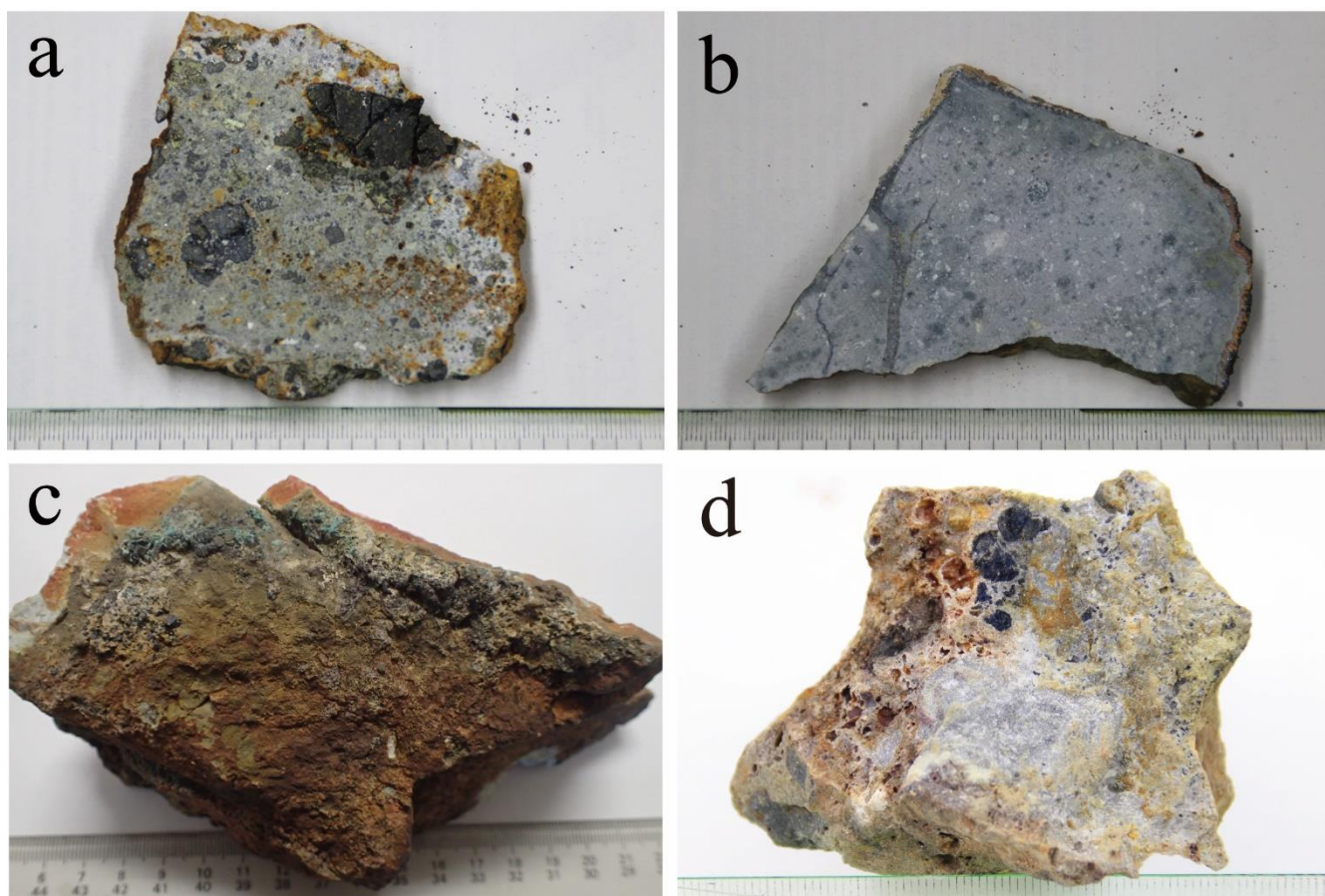


Fig. 4 Representative ore samples from the Murayama and Fukufune mines.

a: Small pyrite grains are disseminated in altered tuff breccia. A weathered rind of variable thickness and brownish reaction halos develop on the ore surface and inside (Murayama mine). b: A silicified and chloritized hard tuff showing a dense and massive inside and a thin red brownish rind on the surface (Murayama mine). c: A well weathered and red brownish colored ore with verdigris on the surface (Fukufune mine). d: A clay-altered and dissolved ore. Fe-hydroxide is deposited on the surface and along fissures, and native sulfur and tenorite (CuO; black) are formed inside (Fukufune mine).

this mine.

Fukufune mine: Most host rocks are strongly chloritized (Fig. 4c) and partly silicified tuffs (Fig. 4d). Ores are composed of chalcopyrite + sphalerite (+pyrite) vein and disseminated chalcopyrite + sphalerite (+pyrite) in brecciated host rocks. The ore samples studied are chalcopyrite-rich by the naked eye. Copper grade in the Fukufune ores is as high as 8.0 to 15.0 %, and a residual copper precipitate was produced during the ore dressing (Yamagata Prefecture, 1977).

Method

Sample Preparation: Ore samples were collected between 2005 and 2014. The samples were cut by diamond-cutter, embedded in polyester resin, and polished using a polishing machine.

pH Measurement: There are many mines and ore deposits in the Nishiyama mining area, including Murayama mine. In order to know the acidity in river water just below the mines, pH of river water was conveniently measured using TES-1380 pH/ORP/Temperature Meter from Oct. 2011 to Sep. 2012.

X-ray Powder Diffraction (XRD) Measurement: Ores and

their weathered rind were shaved using a dental drill, and grinded using agate mortar. Bulk and elutriation (Ethylene glycol and HCl treatments in cases) analyses were done. Measurement equipment and conditions are as follows:

Equipment: RIGAKU MiniFlex II X-ray Diffractometer

Conditions: 30 kV, 15 nA, scanning speed 2°/min, D.S. 0.30 mm, S.S. 1.25°, R.S. 0.30 mm

Measuring range: 2 - 65° (bulk), 2 - 20° (elutriation)

EPMA Measurement: Ore samples were analyzed with a JXA-8900 WDS-type electron microprobe analyzer (EPMA) at the Earth Science Lab. in Yamagata University. Analyses were made for elements Mg, Al, Cd, Zn, S, Si, Na, K, Cu, Fe, P, Ca, Cr, As, Pb, Mn, Ca, Ti, V, Ba and Hg, and instrumental conditions are: 15 kV, 15 nA for quantitative analyses and 20 kV, 50 nA for element mappings.

Results

pH in the rivers

The results of 26 pH measurements of river water are shown in Fig. 2. The data range widely from pH 3.7 to 9.0. The downstream

Table 1 XRD results of ore wastes from the Murayama and Fukufune mines.

Secondary		Murayama (Mry)				Fukufune (Fkf)			
Mineral	Composition	Sph-rich ore	Py-rich ore	Disseminated ore	Cpy-Sph-rich ore	Sph-rich ore	Cpy-Sph-rich ore black	Cpy-Sph-rich ore green	Cpy-Sph-rich ore yellow
Primary	Quartz	SiO ₂	+++	+++	+++	+++	+++	+++	+++
	Chalcopyrite	CuFeS ₂			++	++	++	++	++
	Pyrite	FeS ₂	++	+++	++	+++	++	++	++
	Sphalerite	ZnS	++		+++	+++	+++	+++	+++
	Galena	PbS			++	+++		++	
Secondary	Covellite	CuS				++		++	
	Cupric Sulfate	CuSO ₄ ·xH ₂ O					++*2	*2	
	Anglesite	PbSO ₄			++	++	++		
	Barite	BaSO ₄				++			
	Alunite	KAl(SO ₄) ₂ (OH) ₆			++				
	Jarosite	KFe(SO ₄) ₂ (OH) ₆		++	++	++			+
	Langbeinite	K ₂ Mg ₂ (SO ₄) ₃				++			+
	Halotrichite	FeAl ₂ (SO ₄) ₄ ·22H ₂ O							+
	Plumbojarosite	PbFe ₆ (SO ₄) ₄ (OH) ₁₂		++	++	++			++
	Beaverite	PbCu(Fe,Al) ₂ (SO ₄) ₂ (OH) ₆		+	++	++			++
	Kintoreite	PbFe ₃ (PO ₄) ₂ (OH) ₆			++	++			
	Plumbogummite	PbAl ₃ (PO ₄) ₂ (OH) ₅ ·H ₂ O		++		++			
	Native Sulfur	S				+			
	Goethite	FeO(OH)		+					
	Lepidocrocite	FeO(OH)						+	
	Chlorite		++	++	+		++	++	
	Kaolinite			+	+				++
Others			*1	*1			*3	*4, 5	*4, 6

1: Marcasite FeS₂2: Brochantite Cu₄SO₄(OH)₆

3: Tenorite CuO

+++ : abundant, ++ : common, + : rare (The most intense reflection of each mineral shows 1000 cps <+++ , 100 < ++ < 1000 cps, + < 100 cps.)

4: Mbobomkulite (Ni,Cu)Al₄((NO₃)₂, (SO₄))(OH)₁₂·3H₂O5: Diadochite Fe₂(PO₄)(SO₄)(OH)·5H₂O

6: Nantokite CuCl

points just below the San-ei, Takahi and Miharu mines are as low as 4.3, 3.7 and 4.3, respectively. The cause of these low pH values must be the inflow of acidic materials from the mines. A few points higher than pH 7.0 may result from the excessive neutralization treatment. All five streams studied here are flowing into the Sagae-gawa River, and the pH values at the mouth of the five streams are higher than 5.6 (Fig. 2) because of self-purification and interaction with the surrounding rocks.

XRD measurement

Murayama mine: The term primary/secondary minerals is defined in this study as those deposited at a high temperature hydrothermal stage and as altered products at a lower temperature or weathered in the air environment, respectively. The primary minerals in this mine detected by the XRD are pyrite, chalcopyrite and sphalerite. Sulfate minerals as weathered products are jarosite, langbeinite, halotrichite, beaverite and plumbogummite (Table 1). The diffraction peaks distinctive for some sulfate minerals including K, Fe, Al and Pb are characteristic in this mine. Chlorite, one of the primary hydrothermal gangue minerals, is the most common clay mineral, and kaolinite, a weathering product, is rarely included. Goethite is abundant in every sample.

Fukufune mine: As a primary mineral, sulfides of pyrite, chalcopyrite, galena, sphalerite and clay of chlorite are recognized, and sulfates of barite, alunite, jarosite, langbeinite, halotrichite, plumbojarosite, beaverite, diadochite, mbobomkulite and the secondary clay of kaolinite are detected. It is worthwhile to note that alunite, an Al-rich sulfate, is rich in this mine, whereas jarosite, an Fe-rich sulfate, is rich in the Murayama mine (Table 1).

EPMA Results

Murayama mine

Fe-Cu sulfides: Two types of phase changes on chalcopyrite are recognized; (1) plumbogummite is surrounded by chalcopyrite with a void layer between them (Figs. 5, 6a), (2) Fe-hydroxide surrounds the chalcopyrite directly, with a void layer encompassing the Fe-hydroxide layer (Fig. 6b). The void layer is characteristic in both cases. The sequence from inside to outside in case 1 is chalcopyrite -> void -> plumbogummite, in case 2 it is chalcopyrite -> Fe-hydroxide -> void. This void might be a Fe- or Cu-sulfate such as highly soluble brochantite, and after depositing in a weathering rind, it might have been dissolved in the rain or during the specimen preparation in the laboratory (as discussed later).

Pyrite coexisting with chalcopyrite also has a void layer, which

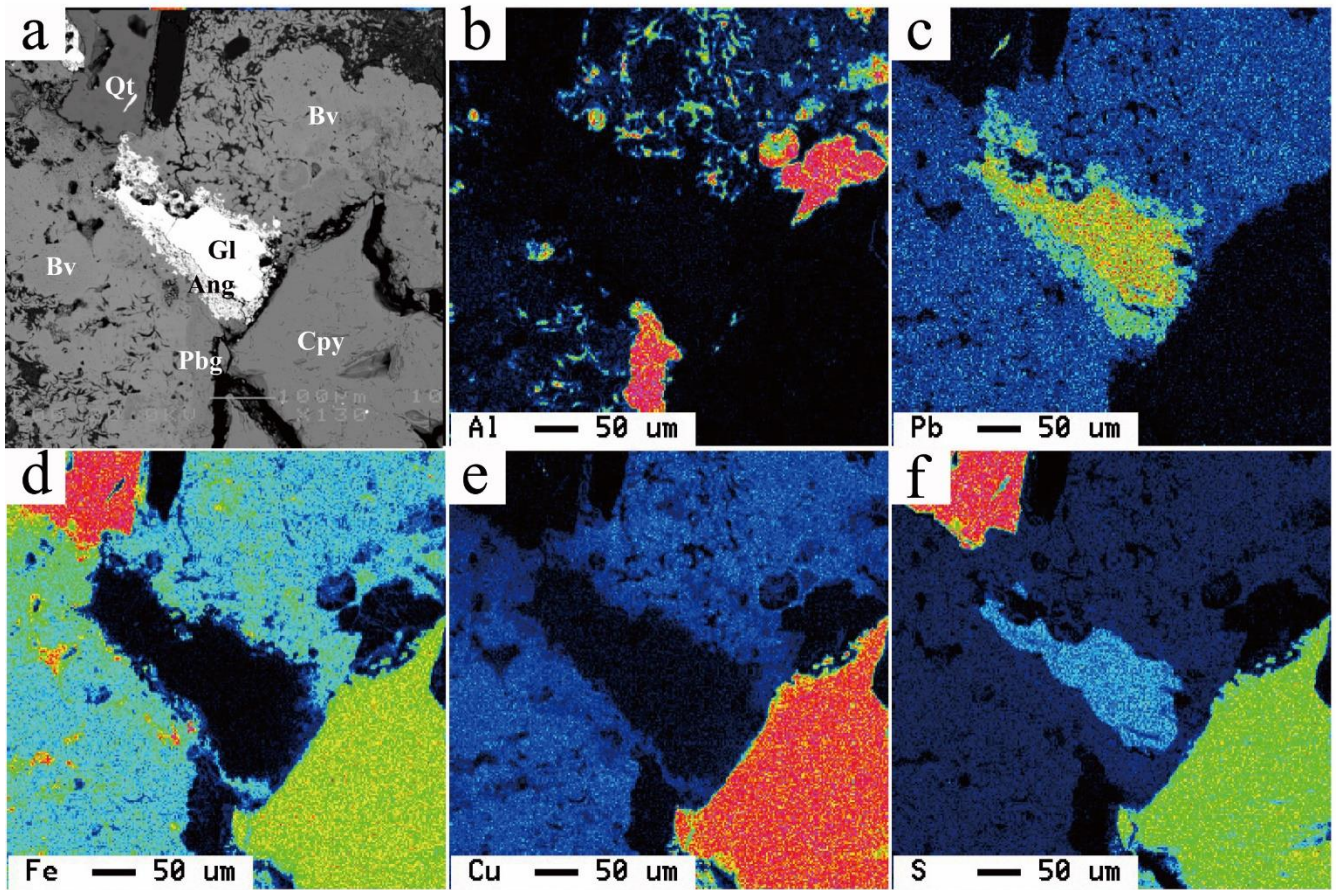


Fig. 5 Alteration of chalcopyrite and galena in the Murayama mine. BSE (Back-scattered electron) image (a) and elemental mappings (b-f). Abbreviations: Ang: anglesite, Bv: beaverite, Cpy: chalcopyrite, Gl: galena, Pbg: plumbogummite, Qt: quartz.

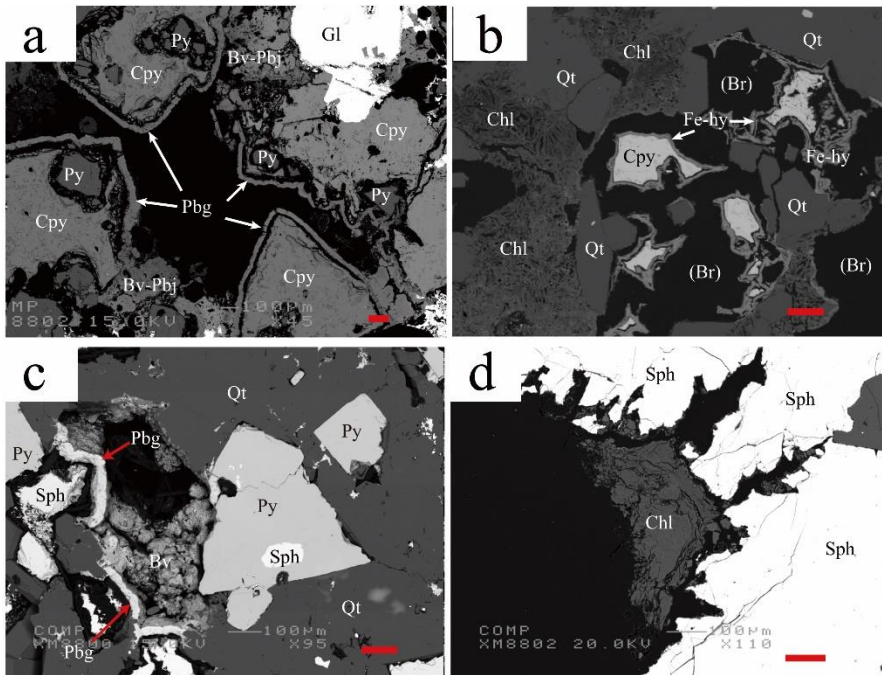


Fig. 6 BSE images showing weathering of major sulfide minerals (Murayama mine) a: Void layers (VL) develop between chalcopyrite (+pyrite) and plumbogummite. b: Chalcopyrite is covered with Fe-hydroxide, and void layers develop outside. c: Pyrite decomposes to beaverite and plumbogummite in a cavity, whereas it included in quartz remains fresh. d: Sphalerite decomposes along outer edges and cracks. Red bars represent 100 μ m. Abbreviations: Bv: beaverite, Chl: chlorite, Cpy: chalcopyrite, Fe-hy: Fe-hydroxide, Gl: galena, Pbg: plumbogummite, Pbj: plumbojarosite, Py: pyrite, Qt: quartz, Sph: sphalerite, VL: void layers.

is surrounded by plumbogummite (Fig. 6a). Beaverite and plumbogummite were deposited in a void in contact with pyrite, whereas pyrite included in quartz remains fresh (Fig. 6c).

Galena: In most cases, anglesite surrounds galena (Fig. 5), therefore, it has been changed directly from galena. In many cases, Pb-bearing sulfates of beaverite and plumbogummite crystallize

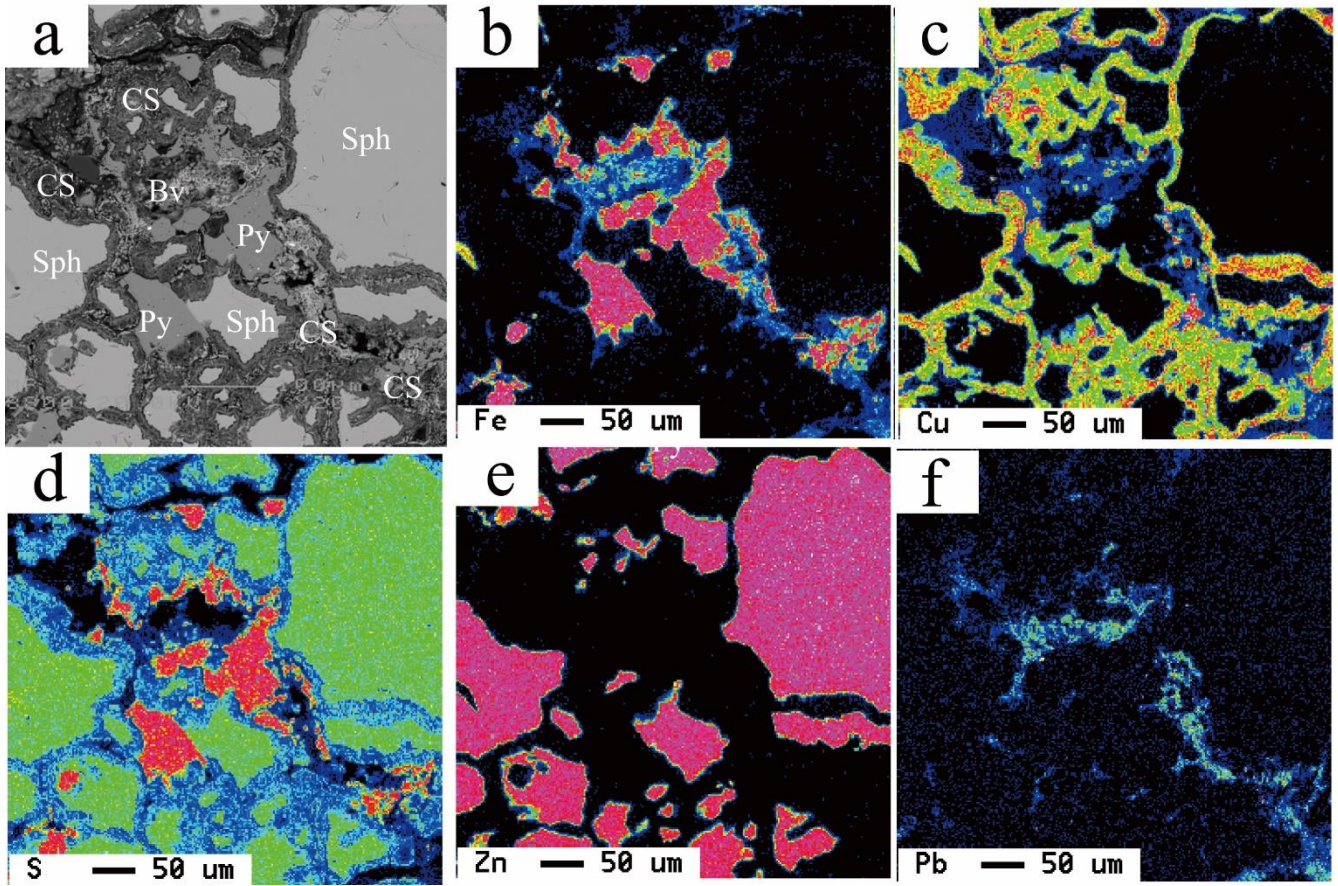


Fig. 7 Alteration of sphalerite and pyrite in the Fukufune mine samples. BSE image (a) and elemental mappings (b-f) showing sphalerite and pyrite decomposing on their periphery, Cu-sulfates enveloping them, and beaverite depositing in the cavity. Abbreviations: Bv: beaverite, CS: Cu-sulfates, Py: pyrite, Sph: sphalerite.

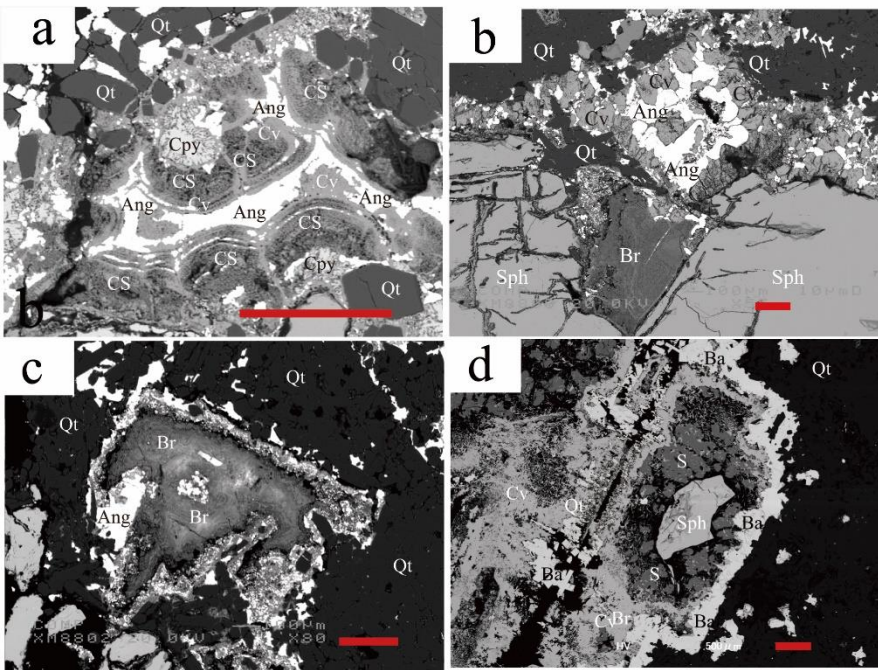


Fig. 8 BSE images showing weathering of major sulfide minerals (Fukufune mine)
a: Covellite and Cu-sulfates surround chalcopyrite, and anglesite fills in the cavity. b: Euhedral covellite crystallizes along the inner rim of the cavity and anglesite fills among the crystals. c: Chalcopyrite decomposes to brochantite. d: Euhedral small grains of barite crystallize along the rim of sphalerite and native sulfur deposits among them. Abbreviations: Ang: anglesite, Ba: barite, Br: brochantite, Cpy: chalcopyrite, CS: Cu-sulfates, Cv: covellite, Qt: quartz, S: native sulfur, Sph: sphalerite. Red bars represent 100 μ m.

outside of anglesite (Fig. 5). This sequence means that the formers were formed after the deposition of the latter. In this case, the texture of anglesite has become disordered and dissolved (Figs. 5a, c).

Sphalerite: Sphalerite decomposes along its outer edge and cracks. There are no secondary minerals including Zn (Fig. 6d).

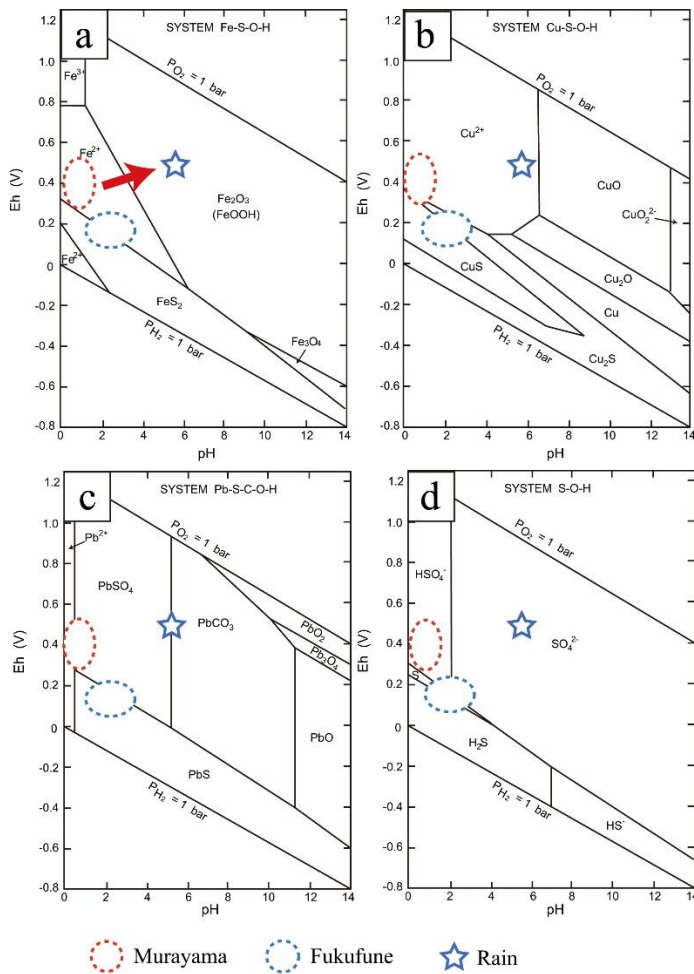


Fig. 9 Eh-pH diagrams showing the representative weathering conditions of the Murayama and Fukufune mines (modified after Brookins, 1988)

a: Fe-S-O-H system ($\text{Fe}=10^{-6}$, $\text{S}=10^{-3}$ M). Much goethite (FeOOH) was produced by the oxidation and increase in pH (arrow; see text). b: Cu-O-H-S system ($\text{Cu}=10^{-6}$, $\text{S}=10^{-3}$ M). Covellite is abundant in the Fukufune mine. c: Pb-S-C-O-H system ($\text{Pb}=10^{-6}$, $\text{S}=10^{-3}$, $\text{C}=10^{-3}$). A part of anglesite (PbSO_4) dissolves in the Murayama mine. d: S-O-H system ($\text{S}=10^{-3}$ M). Native sulfur occurs in the Fukufune mine.

Fukufune mine

Fe-Cu sulfides: Chalcopyrite is strongly weathered in this mine, and covellite and Cu-sulfates (CS) develop around the chalcopyrite (Figs. 7, 8a). The light and shade gradations of CS in Fig. 8a might correspond to water ratios (n-value) in crystals ($\text{CuSO}_4 \cdot n\text{H}_2\text{O}$); light tone to lower water ratios and dark tone to higher water ratios. The CS coincides with brochantite as a result of XRD (Table 1).

Pyrite decomposes on the periphery to be an irregular shape, and CS usually deposits around pyrite (Fig. 7).

Galena: Most of the galena decomposed to anglesite having no trace of its original form (Fig. 8a, 8b, 8c). Anglesite fills the voids among covellite and CS (Fig. 8a), and this means it formed after these Cu-bearing secondary phases.

Sphalerite: Native sulfur deposits around sphalerite, and barite and covellite crystallized around native sulfur (Fig. 8d). Sphalerite decomposed on the periphery and along cracks (Fig. 8b), and there is no Zn-bearing secondary phase around sphalerite.

Discussions

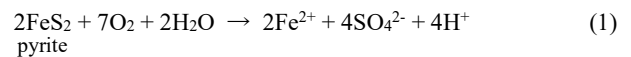
The alteration mode of representative minerals are as follows.

Pyrite

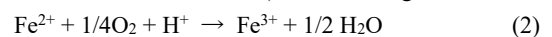
Pyrite is abundant in the Murayama mine whereas chalcopyrite

is abundant and pyrite is scarce in the Fukufune mine (Table 1). This affects the variety of minerals especially sulfates: jarosite, a Fe-K-bearing sulfate, is rich in the Murayama mine, whereas covellite (CuS) and brochantite, a Cu-bearing sulfate, is abundant in the Fukufune mine (Table 2).

Pyrite produces a large amount of H_2SO_4 (H^+ , SO_4^{2-}) during the weathering process via the following reaction (1) (Younger et al., 2002);



This H_2SO_4 component lowers the pH of interstitial waters in the weathered rind. The ferrous (Fe^{2+}) iron in the product changes easily to ferric (Fe^{3+}) iron in the air environment (Reaction 2; Seal and Hammarstrom, 2003), and thereafter ferric iron changes to goethite on contact with rain water (Reaction 3; e.g., Jamber, 2003).



This reaction proceeds by the increase of pH and oxidation (arrow in Fig. 9a). Abundant goethite in the Murayama mine resulted from the decomposition of a lot of pyrite by these processes. On the other hand, goethite is scarce in the Fukufune mine, this derives from the poor amount of pyrite. When the low amount of pyrite decomposes,

Table 2 Summary of the weathering processes of the Murayama and Fukufune mines.

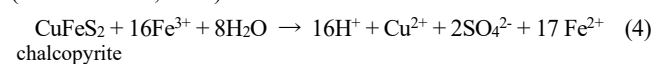
	Murayama Mine	Fukufune Mine
Pyrite	Pyrite ↓ FeSO_4 (?) Fe^{2+} , SO_4^{2-} ↓ Goethite, Fe-hydroxide, Jarosite	Pyrite ↓ dissolved Fe^{2+} , SO_4^{2-}
Galena	Galena ↓ Anglesite (PbSO_4) ↓(dissolved) + Al, P → Plumbogummite + Fe → Plumbojarosite	Galena ↓ Anglesite (PbSO_4) (undissolved)
Chalcopyrite	Chalcopyrite ↓ Cupric sulfate ($\text{CuSO}_4 \cdot n\text{H}_2\text{O}$) ↓ + Pb, Fe, Al → Beaverite	Chalcopyrite ↓ Cupric sulfate ($\text{CuSO}_4 \cdot n\text{H}_2\text{O}$) ⇌ Covellite (CuS)
Sphalerite	Sphalerite ↓ Zn^{2+} , SO_4^{2-} (dissolved)	Sphalerite ↓ Zn^{2+} , SO_4^{2-} ↓ $\text{S}_{(s)}$
Factors	Pyrite-rich, extremely low pH and slightly oxidized	Cu-rich, low pH, reduced

Fe ions are incorporated into sulfates such as beaverite in reaction with Pb, Cu and Al ions (Fig. 7; Table 2). As stated above, decomposition of pyrite produces sulfate ion and Fe^{3+} ion. This Fe^{3+} ion acts as a catalyst to promote the decomposition of other sulfide minerals as follows.

Chalcopyrite

In the Murayama mine, Fe-hydroxides (goethite and amorphous phases) and plumbogummite deposit around the chalcopyrite across a void layer (Fig 6a). This texture indicates highly soluble materials deposited temporarily in the weathered rind. The solubility of Cu- and Fe-bearing sulfates such as chalcantite ($\text{CuSO}_4 \cdot 5\text{H}_2\text{O}$) and melanterite ($\text{FeSO}_4 \cdot 7\text{H}_2\text{O}$) is very high as ca. 20 g/100mL and 26.6 g/100mL at 20°C (Chemical Book). In this case in the Murayama ores, Cu- and/or Fe-bearing sulfates must have deposited around the chalcopyrite, and they dissolved in the rain or during the specimen preparation in the laboratory.

Ferric iron which was produced by the decomposition of pyrite accelerates the decomposition of chalcopyrite as in reaction 4 (Rimstidt et al., 1994).

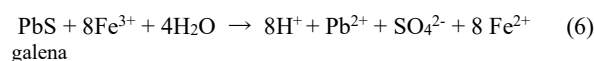


A large amount of covellite (CuS) and cupric sulfate ($\text{CuSO}_4 \cdot n\text{H}_2\text{O}$) precipitates in the Fukufune mine (Fig. 8a, b, d). The Fukufune mine produced copper in great quantity, as copper grade in the crude ore amounts to 8-15 % as described above. Therefore,

cupric sulfates easily precipitated due to the weathering of copper-rich waste. These weathering processes in the Fukufune mine have proceeded under CuS stable conditions as shown in Fig. 9b and Table 2.

Galena

Anglesite usually precipitates around galena, and becomes stable at less than pH 5 (Fig. 9c). Ferric iron also accelerates the decomposition of galena in the same way as chalcopyrite and sphalerite (Reaction 6; Rimstidt et al., 1994).



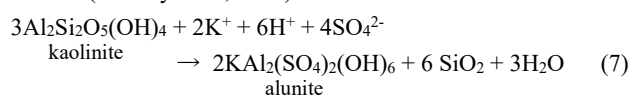
Sulfates

It is worthwhile to note that the occurrence of anglesite in both mines is different; anglesite in the Murayama mine usually shows a porous and dissolved texture (Fig.5), whereas the mineral in the Fukufune mine fills in the void and cracks and shows no dissolved texture. This is the reason for the different pH conditions during weathering processes in both mines; that is, based on the mineral assemblages, anglesite is dissolved in the very low (0-1) pH conditions in the Murayama mine, whereas anglesite and native S remain in the Fukufune mine (pH 2-3) (Fig. 9c, d). This resulted from the different amounts of pyrite; pyrite is very abundant in the Murayama rather than the Fukufune mine. Ferric iron produced by

the decomposition of pyrite accelerates the dissolution of other sulfides, resulting in the generation of voluminous SO_4^{2-} in the Murayama mine.

The difference of pH in both mines affects the occurrence of sulfate minerals other than anglesite; jarosite-series minerals (jarosite, plumbojarosite, plumbogummite and beaverite) are rich in the Murayama mine, whereas alunite is rich in the Fukufune mine. The jarosite-series minerals include Pb, Cu, Fe, Al and P. The very low pH in the Murayama accelerates the decomposition of mafic minerals, feldspars and apatite in host rocks because the solubility of even the highly immobile element Al increases abruptly at low pH (e.g., Stumm and Morgan, 1995).

Alunite is produced by the reaction of kaolinite and SO_4^{2-} as in reaction 7 (Hemley et al., 1969).



Kaolinite is found in both mines (Table 1), and this accelerated the deposition of alunite in acidic conditions. However, the high activity of Pb, Cu, Fe, Al and P in the pore waters in the Murayama mine induced the deposition of jarosite-series minerals instead of alunite.

Summary and Conclusions

Weathering processes of the major sulfide minerals in the Murayama and Fukufune mines are summarized in Table 2.

Pyrite is abundant in the Murayama mine, and the decomposition of pyrite accelerates the dissolution of chalcopyrite, galena and sphalerite, leading to a lowering of pH. The very low pH accelerate the leaching of alkalis, Al and P from the surrounding rocks, and these solutes made jarosite-series mineral with Pb and Cu. Galena changed to anglesite in both mines, but in the Murayama mine, the anglesite changed to plumbojarosite and plumbogummite. Chalcopyrite is small in quantity in the Murayama mine, and this leads to deposition of beaverite in combined with Pb, Fe and Al. On the other hand, chalcopyrite is rich in the Fukufune mine, and abundant covellite and cupric sulfates are attributed to the decomposition of chalcopyrite in this mine.

As stated above, the weathering manner of both mines is different even though they have the same age and similar vein-type deposits. The river waters around the mines become acidic due to the hydrolysis of sulfide minerals. It is important to identify the type of sulfide minerals, especially the amount of pyrite in ores, when treating metal mine drainage. Therefore, estimation of the amount of pyrite leads to proper and safe treating of mine drainage and protection of pollution.

Acknowledgements: We are grateful to Ms. Chiaki Abiko and Saori Kuchiki for the pH measurements in the field and to Dr. Yuya Izumino for the field work. Special thanks are due to Prof. Richard W. Jordan for improving the English manuscript and two anonymous reviewers for their constructive comments of the

manuscript.

References

- Alpers, C.N., Nordstrom, D.K. and Spitzley, J., 2003, Extreme acid mine drainage from a pyritic massive sulfide deposit: The Iron Mountain end-member. *In Jambor, J.L. et al. (eds.) Environmental Aspects of Mine Waste*, Mineralogical Association of Canada, Short Course Series, vol. 31, 407-430.
- Brookins, D.G., 1988, *Eh-pH Diagrams for Geochemistry*. Springer-Verlag, 176p.
- Chemical Book: https://www.chemicalbook.com/ChemicalProductProperty_JP_CB9232125.htm (accessed on 13 October 2017).
- Ghose, M.K., 2002, Air Pollution Due to Opencast Coal Mining and the Characteristics of AirBorne Dust - An Indian Scenario. *International Journal of Environmental Studies*, vol. 59, 211-228.
- Hemley, J.J., Hostetler, P.B., Gude, A.J. and Mountjoy, W.T., 1969, Some stability relations of alunite. *Economic Geology*, vol. 64, 599-612.
- Ito, F., Nomura, T., Katahira, K., Kitagawa, M. and Moriwaki, H., 2010, Influence of pollution from abandoned sulfur mines on riverine environment -Water quality and microbial habitats in Dodo River system-. *Seikatsu Eisei*, vol. 54, 321-329. (in Japanese with English abstract)
- Jambor, J.L., 2003, Mine-waste mineralogy and mineralogical perspectives of acid-base accounting. *In Jambor, J.L. et al. (eds.) Environmental Aspects of Mine Waste*, Mineralogical Association of Canada, Short Course Series, vol. 31, 117-145.
- Kitagawa, R., 2006, Soil pollution in Ashio and Ashio in Ural. *Resource Geology*, vol. 56, 101-109. (in Japanese)
- Lindahl, J., 2014, Environmental impacts of mining in Zambia: Towards better environmental management and sustainable exploration of mineral resources. *SGU (Sveriges Geologiska Undersokning) rapport*, vol. 22, 1-26.
- Matsumoto, S., 2010, Overview of soil pollutions in Japan. *Earth Environment*, vol. 15, 31-35. (in Japanese with English abstract)
- METI (Ministry of Economy, Trade and Industry, 2012) A new guideline for the pollution control project of abandoned mines. (Interim Report). *Workshop for Counterplan of Pollution Control in Abandoned Mines*, 35 p. (in Japanese)
- Otsu, H., 1956, Mineralization and fissure system in the central mining district of Yamagata Prefecture, with special reference to genesis of epithermal veins. *Mining Geology*, vol. 6, 13-24. (in Japanese with English abstract)
- Rimstidt, J.D., Chermak, J.A. and Gagen, P.M., 1994, Rates of reaction of galena, sphalerite, chalcopyrite and arsenopyrite with Fe(III) in acidic solutions. *In C.N. Alpers and D.W. Blowes (eds.) Environmental Geochemistry of Sulfide Oxidation*, American Chemical Society, Symp. Ser. 550, 2-13.
- Seal, R.R. and Hammarstrom, J.M., 2003, Chapter 2. Geoenvironmental models of mineral deposits: Examples from massive sulfide and gold deposits. *In Jambor, J.L. et al. (eds.)*

- Environmental Aspects of Mine Waters*, MAC Short Course Series, vol. 31, 11-50.
- Shoji, K. and Sugai, M., 1992, Chap. 1: The Ashio copper mine pollution case: The origins of Environmental Destruction. In *Ui, J. (ed.) Industrial Pollution in Japan*, 18-63, United Nations University Press.
- Singh, G., 2006, An index to measure depreciation in air quality in some coal mining areas of Korba Industrial Belt of Chhattisgarh, India. *Environmental Monitoring and Assessment*, vol. 122, 309-317.
- Stumm, W. and Morgan, J.J., 1995, *Aquatic Chemistry: Chemical Equilibria and Rates in Natural Waters, 3rd Edition*. Wiley, 1040 p.
- Trivedi, R., Chakraborty, M.K., Sangode, A.G. and Tewary, B.K., 2010, A study of air pollution load assessment around opencast coal project in India, *IJEP (International Journal of Environment and Pollution)*, vol. 30, 198-206.
- Yamagata Prefecture, 1977, *Yamagata-ken Kozanshi (Mining Records of Yamagata Pref.)*, 243 p. (in Japanese)
- YOC (Yamagata Oyo Chishitsu), 2016, *Explanatory leaflet of Geological Map of Yamagata Prefecture*, Yamagata University Press, 62 p. (in Japanese)
- Younger, P.L., Banwart, S.A. and Hedin, R.S., 2002, *Mine Water*. Kluwer Academic Pub., 442 p.

日本語要旨：

陸上鉱山のズリ風化に伴う鉱物相変化：山形県内の2鉱山の比較

林 世峻¹・初川 悠²・中島和夫³・湯口貴史⁴

1: 地盤試験所(株) 〒130-0022 東京都墨田区江東橋 1-16-2

2: 山形大学大学院理工学研究科 〒990-8560 山形市小白川町 1-4-12

3: (株) ASN 〒989-3204 仙台市青葉区南吉成 6-6-3 LABO・CITY 仙台 1F

4: 山形大学理学部 〒990-8560 山形市小白川町 1-4-12

本研究では、鉱山のズリから採取した鉱石について、表面の風化過程を観察し、分解と溶脱の過程を調査した。試料は山形県の西川町、西山鉱床地域に位置する代表的な村山鉱山と尾花沢市福舟鉱山の二つの鉱床の鉱石を扱い、XRD・EPMA 分析と河川の pH 測定を行い、比較検討をした。村山鉱山では、豊富な黄鉄鉱が分解されることで黄銅鉱、方鉛鉱、閃亜鉛鉱などの分解が進み、それに伴い pH が下がることで Al が溶出して鉄明礬系鉱物が多く生じていた。一方、福舟鉱山では黄銅鉱が多く、その分解によって銅藍や硫酸銅が多く沈殿していた。

同時代の同じ鉱脈型鉱床であっても風化の様子が異なっており、これらの違いは鉱石中の硫化物・脈石鉱物の組合せに大きく関係している。周辺の河川水は、鉱石ズリの含 Fe 鉱物の加水分解反応や、それに伴う硫化物の分解により大きく酸性へと変化することが分かった。鉱山の処理計画を立てるには、特に黄鉄鉱の量に注目すべきである。